Evolution Strategy-Based Many-Objective Evolutionary Algorithm Through Vector Equilibrium

Kai Zhang, Zhiwei Xu, Shengli Xie, *Fellow, IEEE*, and Gary G. Yen, *Fellow, IEEE*

***Abstract*—In recent years, numerous many-objective evolutionary algorithms (MaOEAs) have been developed to search for well-diversified and well-converged Pareto optimal solutions for high-dimensional many-objective optimization problems (MaOPs). However, existing MaOEAs have to tackle some daunting challenges, including the emergence of dominance resistance solutions, effective diversity preservation scheme, management of a large population size, extremely high computational complexity, sensitivity to the shape of Pareto front (PF), and overly relying on high-quality reference points. In this article, we present an evolution strategy (ES) for solving MaOPs, called *MaOES*, which can solve these challenges efficiently and effectively. Inspired by the Vector Equilibrium phenomenon in magnetic fields, isotropic magnetic particles would automatically repel from each other, keep the uniform distance from the nearest neighbors, and extend the entire magnetic fields as far as possible, all at the same time. In the proposed algorithm, an efficient self-adaptive Precision-Controllable Mutation operator is designed for individuals to explore and exploit the decision space. In addition, the Maximum Extension Distance strategy, which emulates the isotropic magnetic particle behavior in a magnetic field, is developed to guide individuals to keep uniform distance and extension to approximate the entire PF. As a result, the *MaOES* can obtain a well-converged and well-diversified PF with much less population size and far lower computational complexity. The larger the number of individuals, the sharper the contour the resulting approximate PF will be. Finally, the proposed algorithm is evaluated by the scalable MaOPs test suites on DTLZ and WFG. The experimental results have been demonstrated to provide a competitive and oftentimes better performance when compared against some chosen state-of-the-art MaOEAs.**

***Index Terms*—Evolution strategy (ES), many-objective evolutionary algorithm (MaOEAs), many-objective optimization problem (MaOPs).**

Manuscript received August 5, 2019; accepted December 12, 2019. This work was supported by the National Natural Science Foundation of China under Grant 61472293, Grant 61702383, Grant U1803262, and Grant 61602350. This article was recommended by Associate Editor Q. Zhang. *(Corresponding author: Gary G. Yen.)*

Kai Zhang is with the School of Computer Science and Technology, Wuhan University of Science and Technology, Wuhan 430065, China (e-mail: zhangkai@wust.edu.cn).

Zhiwei Xu is with the Hubei Province Key Laboratory of Intelligent Information Processing and Real-Time Industrial System, Wuhan University of Science and Technology, Wuhan 430065, China (e-mail: kenxucn95@gmail.com).

Shengli Xie is with the Key Laboratory of Intelligent Detection and The Internet of Things in Manufacturing, Ministry of Education, Guangzhou 510006, China, and also with the Guangdong-Hong Kong-Macao Joint Laboratory for Smart Discrete Manufacturing, Guangdong University of Technology, Guangzhou 510006, China (e-mail: shlxie@gdut.edu.cn).

Gary G. Yen is with the School of Electrical and Computer Engineering, Oklahoma State University, Stillwater, OK 74078 USA (e-mail: gyen@okstate.edu).

Color versions of one or more of the figures in this article are available online at http://ieeexplore.ieee.org.

Digital Object Identifier 10.1109/TCYB.2019.2960039

I. Introduction

MANY real-world problems involve multiple conflicting objectives that need to be optimized simultaneously. In the last decades, some of the carefully crafted multiobjective evolutionary algorithms (MOEAs), such as NSGA-II [1] and SPEA2 [2], have shown an extraordinary ability to search for a set of well-converged and well-diversified nondominated solutions in two- or three-objective optimization problems. However, these effective MOEAs fail in tackling real-world applications involving four or many more objectives optimization, such as engineering design [3], air traffic control [4], auto controller [5], and nursing staff scheduling [6].

In recent years, some state-of-the-art designs on many-objective evolutionary algorithms (MaOEAs) have been proposed for solving many-objective optimization problems (MaOPs), including improved diversity-based approaches (e.g., GrEA [7]), enhanced dominance-based approaches (e.g., FD-NSGA-II [8]), decomposition-based approaches (e.g., NSGA-III [9], MOEA/DD [10]), indicator-based approaches (e.g., HypE [11]), objective reduction-based approaches (e.g., PCSEA [12]), and evolution strategy (ES)-based approaches (e.g., S3-CMA-ES [13]). However, when the number of objectives increases, an enormously large number of solutions becomes nondominated. These dominance resistance solutions seriously weaken the selection pressure toward the Pareto front (PF), and the convergence ability of most of the MaOEAs quickly deteriorates. In order to maintain a set of well-diversified solutions which approximates the entire PF, some of the MaOEAs need to increase the number of reference points or the number of search directions, or keep the extreme solutions to extend the boundary. However, without any priori PF shape knowledge, it is very difficult to generate high-quality reference solutions or identify the boundary solutions for high-dimensional MaOPs.

ES has been proven for years to be a simple, yet powerful approach for the optimization problems in particular because of its self-adaptation mechanisms [14], [15]. The ES has been widely applied for solving various multiobjective optimization problems. In order to obtain well-diversified solutions, many diversity approaches have been well integrated into ES, such as niching [16], crossover-like mutation [17], clustering [18],

and archiving [19], [20], to name a few. However, most of these designs still need to maintain a large population size for sorting, selection, and reproduction. In addition, the excessive success of the genetic algorithms (GAs) has inadvertently led to the lost attention on the powerful ES.

In this article, we propose a novel ES for solving MaOPs, called MaOES. In 1917, Richard Buckminster Fuller discovered the significance of vector symmetry and called it the Vector Equilibrium in 1940 [21], [22]. Inspired by the Vector Equilibrium phenomenon in magnetic fields, isotropic magnetic particles would repel each other and extend to the entire magnetic fields as far as possible and automatically. Under this spirit, the proposed MaOES can obtain a well-converged and well-diversified PF with much less population size and far lower computational complexity. The larger the number of individuals, the sharper the contour the resulting approximate PF will be. The proposed algorithm uses mutation and selection for individual self-adaptation. The Precision Controllable Mutation operator is designed for individuals to explore and exploit the decision space efficiently. The Maximum Extension Distance strategy is tailored to guide the individuals to keep uniform distance among particles in the population and to facilitate the extension to approximate the entire PF automatically.

The remaining sections complete the presentation of this article. Section II provides a comprehensive analysis of the existing MaOEAs. The proposed ES for MaOPs and *MaOES* is then detailed in Section III. In Section IV, we elaborate on the experimental results given selected benchmark test problems. Finally, conclusions are drawn in Section V along with pertinent observations that are identified.

II. Literature Review

The mathematical model of an MaOP can be formulated as follows:

$$\min f(x) = \min\left[f_1(x), f_2(x), \ldots, f_M(x)\right]^T, f(x) \in R^M \quad (1)$$

where $x = [x_1, x_2, \ldots, x_N]^T \in \Omega$, and x consists of N decision variables, Ω is the search space. $f(x)$ consists of M objective functions, $f_i(x)$, $i = 1, \ldots, M$ and $M > 3$. R^M denotes the objective space.

In recent years, a number of novel and effective algorithms for MaOPs have been proposed, such as particle swarm optimization with a balanceable fitness estimation for many-objective optimization [23], many-objective optimization using differential evolution with variable-wise mutation restriction [24], MaOEA using a one-by-one selection strategy [25], and set-based GA for interval many-objective optimization problems [26]. Existing strategies of MaOEAs can be broadly classified into several different categories, including improved diversity approaches, enhanced dominance approaches, decomposition-based approaches, indicator-based approaches, objective reduction approaches, and ES-based approaches.

A. Existing Strategies for MaOEAs

1) Improved Dominance or Diversity Approaches: The enhanced dominance approaches, such as FD-NSGA-II [8] and ε-MOEA [27], replace the exact Pareto dominance with some relax dominance definitions, which can enhance the selection pressure toward the PF.

The improved diversity approaches, including GrEA [7] and SPEA2 + SDE [28], attempt to improve the performance of MaOEAs by reducing the adverse impact of diversity maintenance.

However, the delicate balance between convergence and diversity is indeed difficult to maintain throughout the evolution process for these MaOEAs. Excessive aggressive selection pressure may result in degraded diversity maintenance. On the other hand, excessive diversity selection may deteriorate the convergence performance.

2) Decomposition-Based Approaches: The decomposition-based MaOEAs are characterized by systematically generating uniformly distributed normalized weight vectors or reference points. These approaches search for Pareto optimal solutions along each reference vector or reference point. The representative designs include MOEA/DD [10], NSGA-III [9], and RPD-NSGAII [29].

However, the decomposition-based MaOEAs have to maintain an exponentially increasing number of search directions given the increasing number of objectives. The decomposition-based approaches often show high sensitivity to the shape of PF [30], especially for those MaOPs with degenerative PFs. In addition, there exists an infinite number of possible shapes of PF surface in high-dimensional objective space. Without *a priori* knowledge of PF hyper-surface, it is very difficult to generate high quality reference solutions for MaOPs.

3) Indicator-Based Approaches: The indicator-based approaches adopt accurate or estimated indicator values to guide the search process for solving MaOPs. This category includes HypE [11] and IBEA [31].

However, the indicator-based MaOEAs do have their own issues. First, the computational cost is very expensive for the exact hypervolume calculation. Second, the indicator-based MaOEAs encounter difficulties to generate a set of uniformly distributed solutions. Third, it remains a challenge to select the most appropriate reference points for various indicator-based MaOEAs.

4) Objective Reduction Approaches: The objective reduction approaches consist of finding the relevant objectives and eliminating the redundant objectives. Typical representatives are PCSEA [12], L-PCA, and NLMVU-PCA [32].

However, these methods can reduce the computational load but potentially lose some information as a result of the reduced objectives. Moreover, such techniques are only applicable to problems having a moderate number of conflicting objectives.

5) Evolution Strategy-Based Approaches: The ES approaches apply the self-adaptive mutation mechanism for solving MaOPs. Specifically, niching or archive maintenance methods are integrated to maintain well diverse solutions. Some popular designs in this category are S3-CMA-ES [13], PAES [20], and SMES [33]. In particular, ES is simpler to implement, it is easier to scale in a distributed setting, and it has fewer hyperparameters to control. This outcome is no surprise because ES resembles simple hill climbing in

a high-dimensional space-based only on finite differences along a few random directions at each step [34].

However, most of these approaches still need to maintain a large population size for sorting, selection, and reproduction, and, as a result, suffer from extremely high computational complexity largely due to the excessive successes of the GA applications; evolutionary strategy has lost its early attention in the community.

B. Motivation

Generally, when the number of objectives increases, existing MaOEAs have to face the following challenges.

1) The number of incomparable, nondominated solutions increases enormously in the dominance resistance phenomenon [35], [36]; these solutions seriously weaken the selection pressure toward the PF.
2) In order to obtain a set of well-diversified solutions that approximates the entire PF, some of the MaOEAs need to keep the extreme solutions to extend the boundary. However, without any prior PF shape knowledge, it is very difficult to identify the extreme or boundary solutions [37].
3) In order to approximate the high-dimensional PF surface, some of the MaOEAs have to maintain a very large population size, which inadvertently led to expensive computational cost [38].
4) Some of the MaOEAs show high sensitivity to the shape of PF (e.g., decomposition-based approaches are sensitive to degenerate PF [30]).
5) Some of the MaOEAs heavily rely upon the availability of high-quality reference points. However, without *a priori* position and shape knowledge of PF hypersurface, it is very difficult, if not impossible, to generate high quality reference solutions for a given MaOPs.

Inspired by the Vector Equilibrium phenomenon in magnetic fields, isotropic magnetic particles would automatically repel each other, naturally preserve uniform distance from the nearest neighbors, and extend the entire magnetic fields as far as possible. In this article, we present an ES for solving MaOPs, called *MaOES*, which can address these challenges listed above efficiently and effectively.

The proposed algorithm imitates the Vector Equilibrium phenomenon of isotropic magnetic particles, which apply a self-adaptive mutation mechanism to guide the individuals to keep uniform distance and extension to approximate the entire PF automatically. The MaOES can obtain a well-converged and well-diversified PF with much less population size, as shown in Fig. 1.

As can be seen from Fig. 1, given different population sizes (30, 50, and 100), MaOES can obtain well-distributed solutions to cover the entire PF, and each individual keeps uniform distance from nearest neighbor solutions. The larger the number of individuals, the sharper the contour of the resulted approximate PF will be preserved.

III. Proposed Algorithm

In this section, the details of the proposed ES MaOEA are presented. Two main procedures are iteratively run for each individual, specifically the Precision-Controllable Mutation operator and the Maximum Extension Distance strategy. The Precision-Controllable Mutation operator is designed for both exploration and exploitation given the designated precision. The Maximum Extension Distance strategy imitates the isotropic magnetic particles in magnetic fields which guide individuals to maintain uniform distance and extension to approximate the entire PF automatically. The computational complexity of the proposed algorithm is $O(MP^2)$, where M denotes the number of objectives, and P is the population size. This is comparable to most state-of-the-art MaOEA designs.

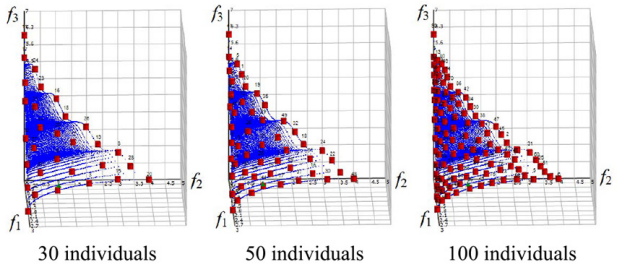

Fig. 1. Resulted approximate PFs by MaOES with different population sizes (30, 50, and 100) on three-objective WFG1.

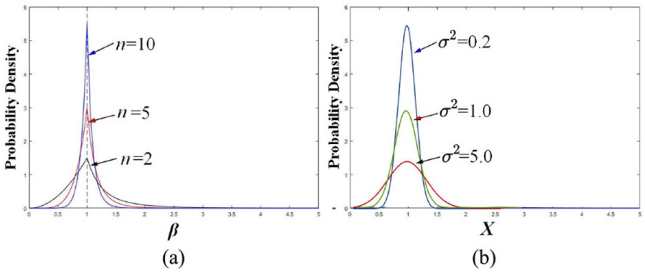

Fig. 2. (a) SBX distributions with different parameter n. (b) Gaussian distributions with different parameter σ.

A. Precision-Controllable Mutation Operator

Let $x = [x_1, x_2, \ldots, x_N]^T$ be one of the individuals, and the x_i is the ith decision variable of x. It is important to exploit the local region near x, and explore the global region distant away from x as well. Traditional mutation operator [39] adopts Gaussian perturbation to generate the mutated candidate solution x_i', as shown in (2)

$$x_i' = x_i + N(0, \sigma). \tag{2}$$

However, the Gaussian distribution is similar to simulated binary crossover (SBX) [40], which generates the offspring near their parent with a high probability, which is only effective for local search, as shown in Fig. 2.

In addition, the Gaussian probability density function has the parameter σ, which is very difficult to be assigned an optimal value. Within limited iteration steps, larger σ value can assure a higher search precision, but slower convergence. On the other hand, smaller σ value can facilitate a quick convergence, but lower search precision. For the WFG instances, all the decision variables are in different ranges $x_i \in [0, 2i]$, which

poses a much difficult task to assign an optimal value of σ specifically suited for all the decision variables simultaneously.

In this article, a simple and efficient Precision-Controllable Mutation operator is proposed for exploration and exploitation, as shown in (3)–(8)

$$x_i' = x_i + \Delta\alpha \tag{3}$$
$$x_i' = x_i - \Delta\alpha \tag{4}$$

where

$$\Delta\alpha = \frac{1}{10^{\text{Random}(p)+1}} \times (\text{Random}(9) + 1)$$
$$x_i' = x_i + \Delta\beta \tag{5}$$
$$x_i' = x_i - \Delta\beta \tag{6}$$

where

$$\Delta\beta = x_i \times \Delta\alpha - x_i$$
$$x_i' = x_i + \Delta\gamma \tag{7}$$
$$x_i' = x_i - \Delta\gamma \tag{8}$$

where

$$\Delta\gamma = x_i \div \Delta\alpha - x_i.$$

Equations (3) and (4) are designed for exploitation, while (5) to (8) are intended for exploration. The variable p is the parameters to control the search precision in the decision space. Function Random(p) can generate a pseudorandom number in the range of 0 to $p-1$. If the required search precision is 0.001, the parameter p can be set to be 3. The value of random number Random(p) should be in the set of {0, 1, 2}, then the corresponding value of $[1/(10^{\text{Random}(p)+1})]$ will be in the set of {0.1, 0.01, 0.001}. The value of (Random(9) + 1) can be regarded as a random coefficient from 1 to 9. Obviously, these mutation equations can generate all the neighboring solutions within the required minimum precision of 0.001.

As an illustrated example, we randomly generate the mutated solution x_i' about 5000 times to test the exploitation ability of (3) and (4). For example, let the original value of x_i be 10, the frequency distribution of mutated x_i is shown in Fig. 3(a) and (b), given the parameter p is set to be 1 and 2, respectively. Please note the addition and subtraction operators are chosen at equal probability. The frequency distribution of newly generated mutated solutions is shown in Fig. 3.

In Fig. 3(a) the parameter p is set to be 1, Random(p) produces a 0, (3) and (4) can generate mutated individual from 9.1 to 10.9 with precision 0.1 of uniform frequency. In Fig. 3(b) the parameter p is set to be 2, Random(p) should be 0 or 1, (3) and (4) can generate uniform spreading mutated solutions near original $x_i = 10$ in precision 0.1 and 0.01.

Equations (5)–(8) can generate new individuals greater than $\Delta\beta$ times or less than $\Delta\gamma$ times of the original x_i, which could be considered exploration the decision space far away from x_i. For example, let x_i be 10, and the parameter p is set to be 1, Random(p) should be 0. We generate mutated x_i' 5,000 times randomly, the frequency distribution is shown in Fig. 4. Equations (7) and (8) can generate mutated solutions with uniform frequency, the value of mutated x_i' become 1 to 10 time more than or less than x_i.

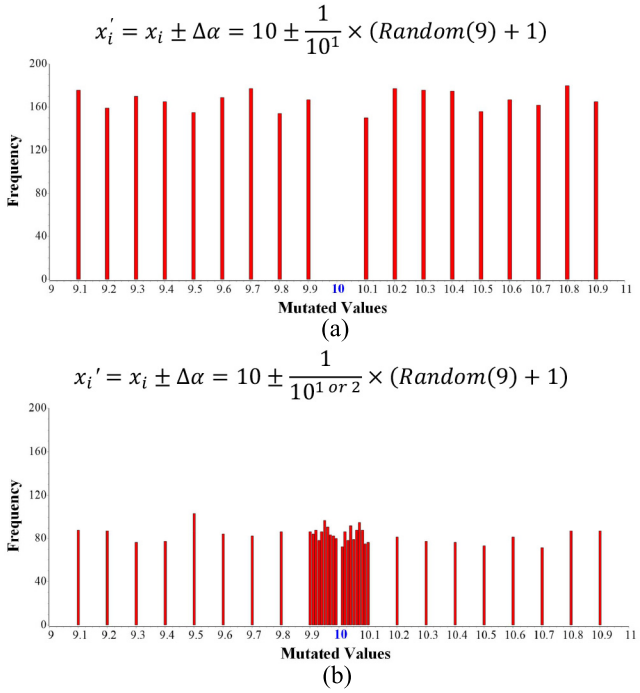

Fig. 3. Frequency distribution of mutated x_i' with different parameter p. (a) $x_i = 10$, $p = 1$, new generated solution x_i' with (3) and (4). (b) $x_i = 10$, $p = 2$, new generated solution x_i' with (3) and (4).

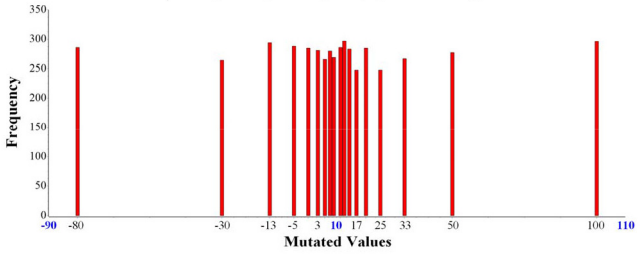

Fig. 4. Value distribution of mutated x_i' with (7) and (8).

Apparently, addition and subtraction mutation operators can generate a small variation $\Delta\alpha$ from its original value, which is useful for local search. On the other hand, division and multiplication mutation operators could generate greater than $\Delta\beta$ times or less than $\Delta\gamma$ times away from the original value, which is useful for global search to jump out of the local optimal. The pseudocode of the Precision-Controllable Mutation is given in Algorithm 1.

B. Maximum Extension Distance Strategy

Since the PF of MaOPs is a high-dimension hypersurface, without any priori PF shape knowledge, it is very difficult to identify boundary solutions for MaOPs. In 1917, Buckminster Fuller discovered the significance of the full vector symmetry in the magnetic fields and called it, the Vector Equilibrium in 1940 [21], [22]. Inspired by the Vector Equilibrium phenomenon, isotropic magnetic particles would repel each other and extend the entire magnetic fields as far as possible. From an energy perspective, the Vector Equilibrium represents the ultimate and perfect condition wherein every isotropic

Algorithm 1 Precision-Controllable Mutation

Input: $P_t^{(i)}$, p=10
Output: $NewP_t^{(i)}$, x_i' is the ith decision variable of $NewP_t^{(i)}$

for $i = 1$ to N
  $x_i' = x_i$
  $r =$ Random(6)
  $\Delta\alpha = \frac{1}{10^{Random(p)+1}} \times (Random(9)+1)$
  $\Delta\beta = x_i \times \Delta\alpha - x_i$
  $\Delta\gamma = x_i \div \Delta\alpha - x_i$
  if $r = 0$ **then** $x_{\text{Temp}} = x_i + \Delta\alpha$
  else if $r = 1$ **then** $x_{\text{Temp}} = x_i - \Delta\alpha$;
  else if $r = 2$ **then** $x_{\text{Temp}} = x_i + \Delta\beta$;
  else if $r = 3$ **then** $x_{\text{Temp}} = x_i - \Delta\beta$;
  else if $r = 4$ **then** $x_{\text{Temp}} = x_i + \Delta\gamma$;
  else if $r = 5$ **then** $x_{\text{Temp}} = x_i - \Delta\gamma$;
  end if
  if x_{Temp} is feasible **then** $x_i' = x_{\text{Temp}}$
end for

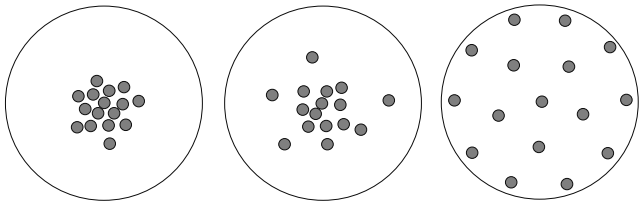

Fig. 5. Isotropic magnetic particles repel each other and expand the boundary automatically. (a) Initial state. (b) Repel each other. (c) Equilibrium state.

magnetic particle keeps uniform distance from the nearest neighbors, as shown in Fig. 5.

In our algorithm, we propose the Maximum Extension Distance strategy to imitate the isotropic magnetic particles behaving in magnetic fields, which guide individuals to preserve uniform distance and extension to approximate the entire PF automatically. The Maximum Extension Distance is defined in (9)

$$\text{MED}\left(P_t^{(i)}\right) = \text{NearDist}\left(P_t^{(i)}\right) \times \text{TotalDist}\left(P_t^{(i)}\right) \tag{9}$$

where

$$\text{NearDist}\left(P_t^{(i)}\right) = \min_{j,j\neq i} \sum_{m=1}^{M} \left| f_m^{(i)} - f_m^{(j)} \right|.$$

$$\text{TotalDist}\left(P_t^{(i)}\right) = \sum_{j=1}^{P} \sum_{m=1}^{M} \left| f_m^{(i)} - f_m^{(j)} \right|.$$

In this equation, $P_t^{(i)}$ is the ith individual in Population P_t at the tth generation. TotalDist($P_t^{(i)}$) calculates the summation of Manhattan distance (MD) between $P_t^{(i)}$ and $P_t^{(j)}$. A greater value of TotalDist($P_t^{(i)}$) implies the solution $P_t^{(i)}$ has moved away from other individuals. NearDist($P_t^{(i)}$) calculates the minimum MD between $P_t^{(i)}$ and $P_t^{(j)}$. A greater value of NearDist($P_t^{(i)}$) implies a better individual diversity. The proposed Maximum Extension Distance strategy is the product of NearDist() and TotalDist(). The greater the maximum extension distance implies an individual has extended the overall boundary, and an individual has obtained a better diversity.

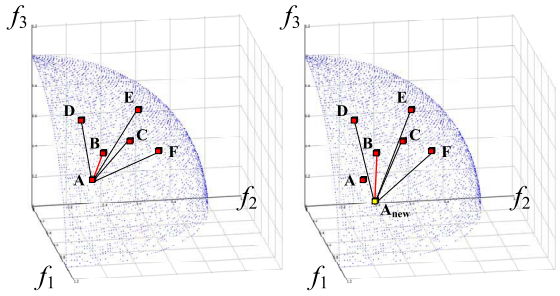

Fig. 6. Maximum Extension Distance to expand the boundary solution.

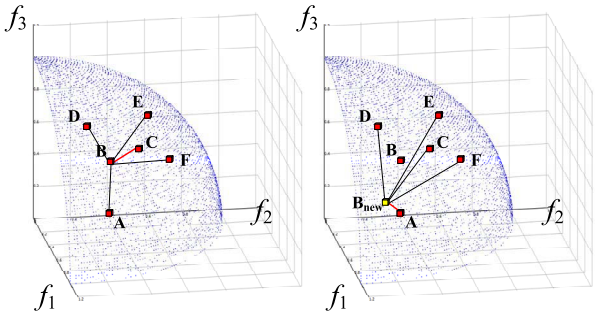

Fig. 7. Maximum Extension Distance to keep good diversity.

For example, the Maximum Extension Distance can expand the boundary solution. Let A be an individual in the population, and A_{new} is the new candidate solution after mutation operation, as shown in Fig. 6.

The Maximum Extension Distance is calculated as follows:

$$\begin{aligned}
\text{MED}(A) &= \text{NearDist}(A) \times \text{TotalDist}(A) \\
\text{NearDist}(A) &= \text{MD}(AB) \\
\text{TotalDist}(A) &= \text{MD}(AB)+\text{MD}(AC)+\text{MD}(AD)+\text{MD}(AE) \\
&\quad +\text{MD}(AF) \\
\text{MED}(A_{\text{new}}) &= \text{NearDist}(A_{\text{new}}) \times \text{TotalDist}(A_{\text{new}}) \\
\text{NearDist}(A_{\text{new}}) &= \text{MD}(A_{\text{new}}B) \\
\text{TotalDist}(A_{\text{new}}) &= \text{MD}(A_{\text{new}}B)+\text{MD}(A_{\text{new}}C)+\text{MD}(A_{\text{new}}D) \\
&\quad +\text{MD}(A_{\text{new}}E)+\text{MD}(A_{\text{new}}F) \\
\text{MED}(A_{\text{new}}) &> \text{MED}(A).
\end{aligned}$$

Compared with the original solution A, both NearDist() and TotalDist() of A_{new} are greater than those of A. Since the Maximum Extension Distance, MED(A_{new}), is greater than the value of MED(A), the individual A should be replaced by the new candidate solution A_{new}. Obviously, A_{new} extends the whole population boundary and extends individual distance far away from other individuals.

For another example, B is an individual in the population, and B_{new} is a new candidate solution after mutation operation, as shown in Fig. 7.

The Maximum Extension Distance is calculated as follow:

$$\text{MED}(B) = \text{NearDist}(B) \times \text{TotalDist}(B)$$

Algorithm 2 Maximum Extension Distance

Input: the index of mutation individual ***idx***
Output: maximum extension distance ***MED***

```
TotalDist = 0;
NearDist = +8;
for i = 1 to P
    if i = idx then continue;
    Dist = 0;
    for j = 1 to M
        Dist = Dist + abs(f_j^(i) − f_j^(idx));
    end for
    TotalDist = TotalDist + Dist;
    if Dist < NearDist then NearDist = Dist;
end for
MED = NearDist × TotalDist;
```

$$\begin{aligned}
\text{NearDist}(B) &= \text{MD}(BC)\\
\text{TotalDist}(B) &= \text{MD}(BA)+\text{MD}(BC)+\text{MD}(BD)+\text{MD}(BE)\\
&\quad +\text{MD}(BF)\\
\text{MED}(B_{\text{new}}) &= \text{NearDist}(B_{\text{new}}) \times \text{TotalDist}(B_{\text{new}})\\
\text{NearDist}(B_{\text{new}}) &= \text{MD}(B_{\text{new}}A)\\
\text{TotalDist}(B_{\text{new}}) &= \text{MD}(B_{\text{new}}A)+\text{MD}(B_{\text{new}}C)+\text{MD}(B_{\text{new}}D)\\
&\quad +\text{MD}(B_{\text{new}}E)+\text{MD}(B_{\text{new}}F)\\
\text{MED}(B_{\text{new}}) &< \text{MED}(B).
\end{aligned}$$

Although TotalDist() of B_{new} are greater than B, NearDist() of B_{new} is far less than that of B. Smaller NearDist() means B has moved closer to other individuals, the diversity would be degenerated. Since the Maximum Extension Distance $\text{MED}(B_{\text{new}})$ is less than the value of $\text{MED}(B)$, individual B should not be replaced by the candidate solution B_{new}. The time complexity of Maximum Extension Distance strategy is $O(MP)$. The pseudocode is given in Algorithm 2.

C. Overall Algorithm

For a given MaOP, a population of randomly sampled individuals are generated. At each generation, the proposed ES adopts the Precision-Controllable Mutation operator to every individual in each decision variant.

Let $P_t^{(i)}$ be the ith original solution in population P_t, and $\text{New}P_t^{(i)}$ be the mutated new solution of $P_t^{(i)}$. If $\text{New}P_t^{(i)}$ dominate $P_t^{(i)}$, the new mutated solution would replace the original one. If $\text{New}P_t^{(i)}$ is dominated by $P_t^{(i)}$, the new mutated solution would be neglected.

If $\text{New}P_t^{(i)}$ and $P_t^{(i)}$ are nondominated with respect to each other, our algorithm would compare the numbers which other solutions in the population that dominate $P_t^{(i)}$ or $\text{New}P_t^{(i)}$. Let $\text{DomCount}(P_t^{(i)})$ be the function that calculate the number of other solutions dominate $P_t^{(i)}$, the computational complexity is $O(MP)$. If the function value of $\text{New}P_t^{(i)}$ become smaller than the value of $P_t^{(i)}$, that is, less solutions can dominate $\text{New}P_t^{(i)}$, the proposed algorithm would accept the new mutated solution. If the value of $\text{DomCount}(\text{New}P_t^{(i)})$ become equal to the value of $P_t^{(i)}$, our algorithm would continue to compare the value of Maximum Extension Distance.

If the value of Maximum Extension Distance $\text{MED}(\text{New}P_t^{(i)})$ is greater than $\text{MED}(P_t^{(i)})$, the new mutated solution is better than the original one, and would replace it. Otherwise, we should eliminate the new solution. The computational complexity of the overall algorithm is $O(MP^2)$. The pseudocode is given in Algorithm 3.

Algorithm 3 Proposed *MaOES* Algorithm

Input:
Output:

```
Initialization P_t, t = 0
while ( t < maximum generation )
    for i = 1 to P
        New P_t^(i) = Precision-Controllable Mutation (P_t^(i))
        Objective Function Calculation (New P_t^(i))
        if (New P_t^(i) ≺ P_t^(i)) then
            P_t^(i) = New P_t^(i)
        else if (New P_t^(i) ⊀ P_t^(i)) and (P_t^(i) ⊀ New P_t^(i)) then
            if DomCount(New P_t^(i)) < DomCount (P_t^(i)) then
                P_t^(i) = New P_t^(i)
            elseif DomCount(New P_t^(i)) = DomCount (P_t^(i)) then
                if MED(New P_t^(i)) > MED(P_t^(i)) then
                    P_t^(i) = New P_t^(i)
                end if
            end if
        end if
    end for
end while
```

IV. Experimental Results

In order to validate the proposed MaOES, we compare its performance with some state-of-the-art representatives from different categories of MaOEAs, including NSGA-III [9], MOEA/DD [10], GrEA [7], HypE [11], RPD-NSGAII [27], S3-CMA-ES [13], MyO-DEMR [24], NMPSO [23], and onebyone EA [25]. In the comparison, these algorithms are evaluated on 16 scalable benchmark instances in WFG [41] and DTLZ [42] suites. These MaOPs contain different problem characteristics, such as convex, concave, disconnected, linear, and degenerated. We perform 30 independent runs for each algorithm on each test instance and the maximum evaluation is set to 10 000.

For the proposed MaOES, the SBX and the polynomial mutation have been adopted for real-coded GAs. For a fair comparison, the population size is set to 200, SBX distribution index is set to 20, polynomial mutation distribution index is set to 20, crossover probability is set to 1.0, and mutation probability is set to $1/N$, where N denotes the number of decision variables. The other variable parameters of the compared algorithms are adopted as suggested in the original papers, including [7], [9]–[11], [13], [23]–[25], and [27].

For each benchmark instance, 10 000 true PF solutions (i.e., PF true), are generated by PlatEMO [43] to evaluate the inverted generational distance (IGD) [44]. The IGD indicator measures the distance between the true PF and the closest individual in the obtained solutions. The indicator can be expressed as

$$I_{\text{IGD}} = \frac{\left(\sum_{i=1}^{|PF|} d_i^2\right)^{1/2}}{|\text{PF}|} \tag{10}$$

TABLE I
AVERAGE IGD VALUES OVER 30 RUNS ON UNCONSTRAINT DTLZ AND WFG BENCHMARK INSTANCES (POPULATION SIZE 200), WHERE THE BEST MEAN FOR EACH INSTANCE IS SHOWN WITH A GRAY BACKGROUND

Problem	*M*	*N*	MaOES	GrEA	NSGA-III	MOEA/DD	HypE	RPD-NSGAII	S3-CMA-ES	MyO-DEMR	NMPSO	onebyone EA
DTLZ1	3	7	0.0138	0.6004+	0.9790+	1.2989+	0.3984+	0.2290+	30.987+	0.0953+	5.1722+	0.3386+
	5	9	0.0528	1.2285+	0.8552+	0.6586+	0.4022+	0.2378+	25.949 +	0.1137+	4.5790 +	0.5562+
	8	12	0.0954	1.7951+	2.0421+	0.5854+	0.4772+	0.3363+	22.108+	0.2609+	4.7884+	0.5980+
	10	14	0.1161	2.3832+	1.5203+	0.3484+	0.4996+	0.4563+	20.223+	0.2779+	5.4433 +	0.4900+
DTLZ2	3	12	0.0356	0.0531+	0.0400+	0.0390+	0.1128+	0.0405+	0.0391+	0.0565+	0.0551+	0.0377+
	5	14	0.1597	0.1788+	0.2018+	0.1968+	0.3337+	0.2020+	0.1704+	0.2152+	0.1904 +	0.1655+
	8	17	0.3294	0.4515+	0.3991+	0.3286=	0.5518+	0.3543+	0.3605+	0.5072+	0.3456 +	0.3322–
	10	19	0.4097	0.4318+	0.5918+	0.4452+	0.7125+	0.4658+	0.4316+	0.7475+	0.4343+	0.4109+
DTLZ3	3	12	0.0393	18.502+	33.536+	41.628+	13.635+	13.141+	242.73+	6.1721+	116.80+	14.833+
	5	14	0.1718	36.176+	30.316+	29.953+	22.777+	15.566+	243.04+	10.639+	142.07 +	20.772+
	8	17	0.3587	102.45+	78.377+	27.984+	32.673+	19.265+	235.19+	16.231+	152.46 +	25.101+
	10	19	0.4549	179.02+	107.06+	14.592+	30.066+	17.980+	241.63+	12.714+	156.60+	25.433+
DTLZ4	3	12	0.0489	0.1189+	0.0408–	0.0398–	0.1432+	0.0414–	0.5918+	0.1329+	0.0575+	0.0552+
	5	14	0.1765	0.1845+	0.2343+	0.2143+	0.3949+	0.2073+	0.6846+	0.3955+	0.1989+	0.1718–
	8	17	0.3305	0.3616+	0.4310+	0.3481+	0.6133+	0.3717+	0.7972+	0.5766+	0.3989+	0.3428+
	10	19	0.4173	0.4400+	0.5600+	0.4818+	0.7123+	0.4919+	0.8633+	0.6502+	0.4759+	0.4335+
DTLZ5	3	12	0.0019	0.0153+	0.0072+	0.0237+	0.0067+	0.0192+	0.0027+	0.0166+	0.0069+	0.0025+
	5	14	0.0427	0.1207+	0.1974+	0.1033+	0.0321–	0.1025+	0.0038–	0.8101+	0.0883+	0.0059+
	8	17	0.0750	0.2490+	0.2477+	0.1601+	0.0449–	0.1754+	0.0082–	1.4461+	0.6628+	0.0077–
	10	19	0.0665	0.3450+	0.3513+	0.2026+	0.0491–	0.1856+	0.0060–	1.7207+	0.8313+	0.0093–
DTLZ6	3	12	0.0019	0.0198+	0.0309+	0.1395+	0.1349+	0.0576+	3.8892+	0.0435+	0.0119+	0.0044+
	5	14	0.0051	0.4223+	2.0510+	0.4040+	0.2135+	0.3322+	3.9544+	0.7684+	0.0338+	0.1086+
	8	17	0.0059	5.1129+	5.7989+	1.0861+	0.2747+	1.2810+	4.1403 +	1.4083+	0.6827+	0.2305+
	10	19	0.0142	2.9786+	6.2149+	0.8684+	0.2920+	1.6775+	4.2038+	1.6278+	0.6930+	0.2765+
DTLZ7	3	22	0.0367	0.0835+	0.1699+	0.4356+	0.7902+	0.0988+	0.1400+	0.3094+	0.0461+	0.1966+
	5	24	0.2191	0.3326+	0.6383+	2.4510+	2.6380+	0.4655+	0.2639+	1.2198+	0.3279+	0.3361+
	8	27	0.5881	1.3453+	5.4781+	1.5915+	5.5394+	3.2216+	0.7368+	8.0621+	0.8794+	0.8919+
	10	29	0.7889	5.6828+	7.2211+	2.2289+	7.2765+	5.4310+	1.0690 +	13.381+	1.1410+	1.5705+
WFG1	3	12	0.0894	1.2363+	1.4147+	1.5000+	1.5593+	1.2117+	1.8200 +	1.9932+	1.5169 +	1.3101+
	5	14	0.3951	1.8257+	1.8599+	2.0573+	1.9290+	1.5084+	2.1818+	2.2603+	1.9804 +	1.8961+
	8	17	0.8825	2.6740+	2.6409+	2.7861+	2.6268+	2.2579+	2.6955 +	2.8188+	2.6274 +	2.5930+
	10	19	1.6422	2.8827+	2.9392+	3.1645+	2.8493+	2.6941+	3.1199+	3.1906+	2.9732 +	2.9700+
WFG2	3	12	0.0703	0.1652+	0.1719+	0.3510+	0.2287+	0.1668+	0.1813+	0.2791+	0.2281+	0.3129+
	5	14	0.3926	0.7136+	0.8093+	3.3112+	1.3503+	0.9122+	1.0606+	0.8330+	0.6477+	0.6675+
	8	17	0.5502	1.4572+	2.5043+	5.1587+	2.8163+	1.9433+	1.2973+	1.5838+	1.2273 +	1.4599+
	10	19	1.9494	2.7855+	6.1756+	11.012+	5.7443+	2.5734+	1.7162–	2.4117 +	1.3395–	1.5670–
WFG3	3	12	0.0079	0.1173+	0.1634+	0.2363+	0.0427+	0.1439+	0.1375+	0.2280+	0.1175+	0.5090+
	5	14	0.0143	0.5059+	0.6020+	0.8114+	0.0739+	0.4965+	0.3536+	0.8639+	0.4110 +	1.6163+
	8	17	0.0235	1.2071+	1.0524+	2.0610+	0.1071+	1.2237+	0.8766+	5.9430+	0.9260+	4.4061+
	10	19	0.0295	1.9284+	1.9483+	3.6206+	0.1315+	2.0853+	1.4151 +	7.8455 +	1.1104+	6.3754+
WFG4	3	12	0.1239	0.1946+	0.1830+	0.1928+	0.2614+	0.1795+	0.3143+	0.2492+	0.2189+	0.3428+
	5	14	0.8943	0.9826+	1.1576+	1.2245+	1.2798+	1.1751+	1.0138 +	1.0960+	1.0665+	1.5021+
	8	17	2.7380	2.7854+	3.0416+	3.5097+	5.3361+	2.9721+	2.9579+	3.0745+	2.8650 +	4.0004+
	10	19	4.2618	4.6595+	5.1635+	5.6819+	8.5389+	5.1197+	4.5069 +	4.7692+	4.3024+	5.9271+
WFG5	3	12	0.1537	0.2136+	0.1947+	0.2132+	0.2928+	0.1865+	0.1750+	0.2157+	0.2234+	0.4447+
	5	14	0.9042	0.9764+	1.1288+	1.2127+	1.3296+	1.1434+	0.9723+	1.0572+	1.0404+	1.5536+
	8	17	2.8501	2.8484=	3.0247+	3.3905+	3.2943+	2.9630+	3.0518+	3.0968+	2.8546 =	4.1923+
	10	19	4.4069	4.3998–	5.0844+	6.3570+	6.0196+	5.2750+	4.4983 +	4.8108+	4.2201–	6.0187+
WFG6	3	12	0.1297	0.2477+	0.2663+	0.2873+	0.3023+	0.2422+	0.1920+	0.3131+	0.3457+	0.5390+
	5	14	0.9096	1.0272+	1.1696+	1.2321+	1.3667+	1.1737+	1.0409 +	1.1289+	1.1762+	1.7776+
	8	17	2.9067	2.8977=	3.0751+	3.3831+	3.4403+	3.0132+	3.1543+	3.0818+	3.0526+	4.5182+
	10	19	4.5476	4.4688+	5.5688+	6.1866+	6.2612+	5.2469+	4.6468+	4.8854+	4.6209+	6.4726+
WFG7	3	12	0.1307	0.2063+	0.1809+	0.2173+	0.3154+	0.1750+	0.7185+	0.2288+	0.2192+	0.4732+
	5	14	0.9358	0.9999+	1.1585+	1.2453+	1.4220+	1.1708+	1.8465 +	1.1006+	1.1011+	1.7590+
	8	17	3.1514	2.8352+	3.0673+	3.2777+	3.9833+	2.9949–	3.6400+	3.0486–	2.9194–	4.0453+
	10	19	4.9429	4.5414+	5.2745+	5.2346+	7.1321+	5.2724+	4.9701+	4.9377=	4.4322–	5.5395+
WFG8	3	12	0.1849	0.2948+	0.3058+	0.3039+	0.3343+	0.3022+	0.3636+	0.3579+	0.3185+	0.5612+
	5	14	1.0654	1.0923+	1.2068+	1.2594+	1.3132+	1.2205+	1.3034+	1.1680+	1.1541+	1.7727+
	8	17	3.1035	3.2130+	3.5399+	3.4012+	4.4315+	3.3562+	3.5534+	3.4163+	3.1630+	3.9956+
	10	19	4.8891	5.7403+	5.7802+	5.6986+	6.7056+	5.4445+	5.0941+	6.6361+	4.6793–	5.6100+
WFG9	3	12	0.1388	0.1962+	0.1830+	0.2100+	0.2729+	0.1842+	0.1564+	0.2174+	0.2498+	0.3256+
	5	14	0.9321	0.9554+	1.1156+	1.2402+	1.2330+	1.1206+	0.9939+	1.0725+	1.0266+	1.4437+
	8	17	2.9575	2.8988–	3.1541+	3.3643+	3.5073+	3.0998+	3.1715+	3.1337+	2.9655=	3.8025+
	10	19	4.6842	4.5127+	5.1564+	5.8263+	6.4678+	5.2846+	4.5663–	4.9428+	4.3932–	5.4122+

where *di* is the Euclidean distance between the *i*th solution in the true PF and the closest individual in the obtained solutions. As a matter of fact, the lower the IGD value is, the better approximate solution set is obtained.

To facilitate the experiments, we have implemented the algorithm in the object Pascal language and developed a graphical user interface (GUI) under the Delphi XE7 platform. The GUI and *MaOES* algorithm source code are available

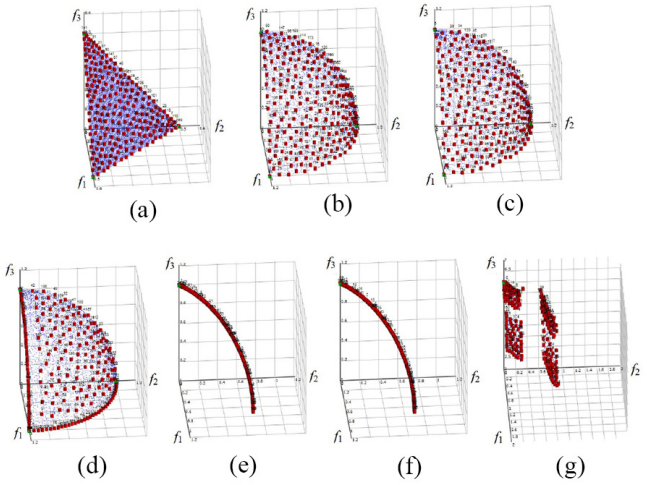

Fig. 8. Experimental results for three-objectives benchmark problems on unconstraint DTLZ suite by MaOES (population sizes 100). (a) DTLZ1. (b) DTLZ2. (c) DTLZ3. (d) DTLZ4. (e) DTLZ5. (f) DTLZ6. (g) DTLZ7.

in the following website: https://github.com/MaOEA/MaOES. Interested readers can retrieve the code and validate the performance on his/her own.

A. Performance on DTLZ Problems

The IGD values obtained by the ten competing algorithms are given in Table I. One can easily notice that MaOES performs significantly better than those of competing MaOEAs on DTLZ1, DTLZ6, and DTLZ7 with respect to all considered numbers of objectives. For DTLZ2, MOEA/DD obtains a better IGD value on the eight-dimension instances while MaOES shows better results with the other DTLZ2 instances. For DTLZ4, MOEA/DD and onebyone EA obtain better IGD values on the 3-objective instance and 5-objective instance, respectively, and MaOES has the best performance when the number of objectives is more than 5. For DTLZ5, S3-CMA-ES and onebyone EA outperform other MaOEAs in almost all DTLZ5 instances, while MaOES wins 3. From 28 test instances of the DTLZ benchmark problems, it is clear that MaOES is the best optimizer as it wins in 22 instances. Thus, from the empirical results on DTLZ1–DTLZ7 test problems, we find that MaOES outperforms other compared MaOEAs.

The results demonstrate the ability of the proposed MaOES to deal with MAOPs characterized by linear, concave, degenerated, and discontinues PFs. For example, given the three-objective DTLZ instances, 100 nondominated solutions over 5,000 generations can be seen in Fig. 8.

Fig. 9 shows the corresponding parallel coordinates of the solutions of MaOES on 10-D DTLZ test instances. In comparison with parallel coordinates of true PF sampled by PlatEMO. As can be seen in Fig. 9, MaOES has a good convergence on DTLZ1-DTLZ4, and DTLZ7. However, MaOES have a poor population convergence on ten-dimension DTLZ5 and DTLZ6. In the DTLZ6 of Fig. 8, some individuals already have obtained good convergence and distribution PF ranging from 0 to 1. Please note that DTLZ5 has a nondegenerate part of the PF, although DTLZ5 has often been used as MaOP with degenerate PFs. Because of the effectiveness of Maximum

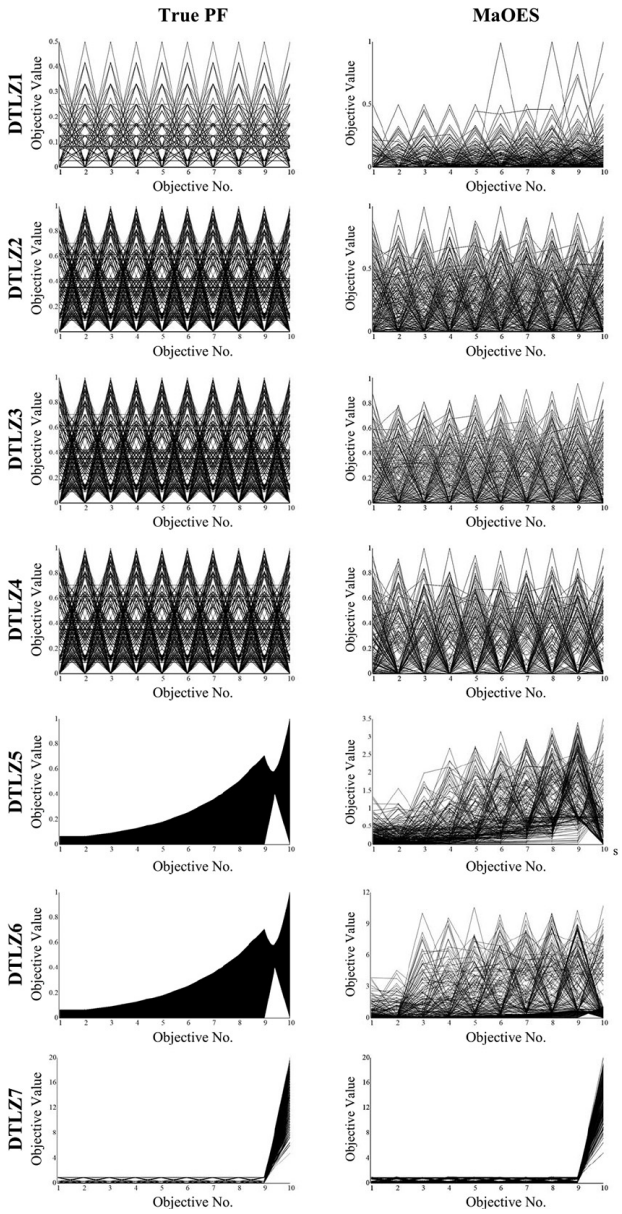

Fig. 9. Solution sets obtained by MaOES and true PF on the ten-objective DTLZ test suite through parallel coordinates.

Extension Distance strategy, MaOES obtain good coverage for all DTLZ test instances, and almost uniformly contribution to all ten objectives.

B. Performance on WFG Problems

As can be seen from Table I, MaOES has better IGD means values than the other MaOEAs in all WFG1, WFG3, and WFG4 instances. For WFG2, WFG5, and WFG8, NMPSO obtains better IGD values on the 10-objective instances and MaOES shows better results with all the remaining instances. For WFG7 and WFG9, GrEA obtains better IGD values on the 8-objective instances, while NMPSO has the best performance on the 10-objective instances. For WFG6, GrEA obtains better IGD values on the 8-objective and 10-objective instances, and MaOES shows better results with the other WFG6 instances.

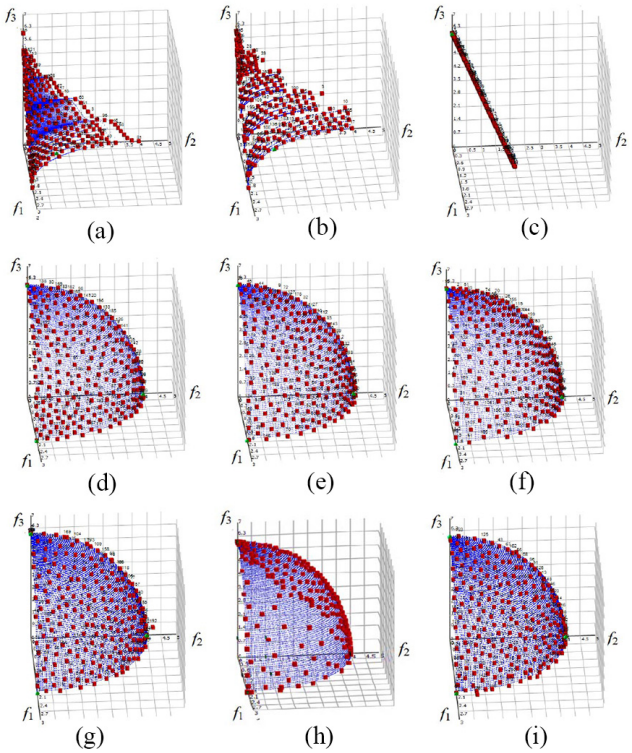

Fig. 10. Experimental results for three-objectives benchmark problems on unconstraint WFG suite by MaOES (population sizes 100). (a) WFG1. (b) WFG2. (c) WFG3. (d) WFG4. (e) WFG5. (f) WFG6. (g) WFG7. (h) WFG8. (i) WFG9.

From the 36 WFG problem instances, MaOES wins in 27 instances which clearly show the ability of the proposed MaOES to deal with MaOPs characterized by mixed convex and concave, disconnected convex, degenerated and concave PFs.

For example, given the three-objective WFG instances, the final nondominated solutions over 5,000 generations can be seen in Fig. 10. Fig. 10(a) shows the proposed algorithm can find well-convergent and well-diversified solutions on mixed convex and concave PF for WFG1. As can be seen from Fig. 10(b), our algorithm obtains a proper distribution among solutions for WFG2 with disconnected convex PF. Fig. 10(c) shows our MaOES can obtain quality convergence and uniform solutions that lie on the degenerated WFG3. Fig. 10(d)–(j) show that the MaOES obtain sets of good distributed solutions that cover the whole concave PFs for WFG4-WFG9.

Fig. 11 shows the corresponding parallel coordinates of the solutions of MaOES on ten-objectives WFG test instances. In comparison with parallel coordinates of true PF sampled by PlatEMO. As can be seen in Fig. 11, MaOES has a good convergence on eight WFG test instances (i.e., WFG1 and WFG3-WFG9). In addition, our proposed algorithm obtains a uniform coverage for each objective, largely due to the effective design of Maximum Extension Distance strategy. However, MaOES fails to cover the region on the first three objectives for WFG2, and there are no solution distributed in the second objective ranging from 2 to 4 for WFG8.

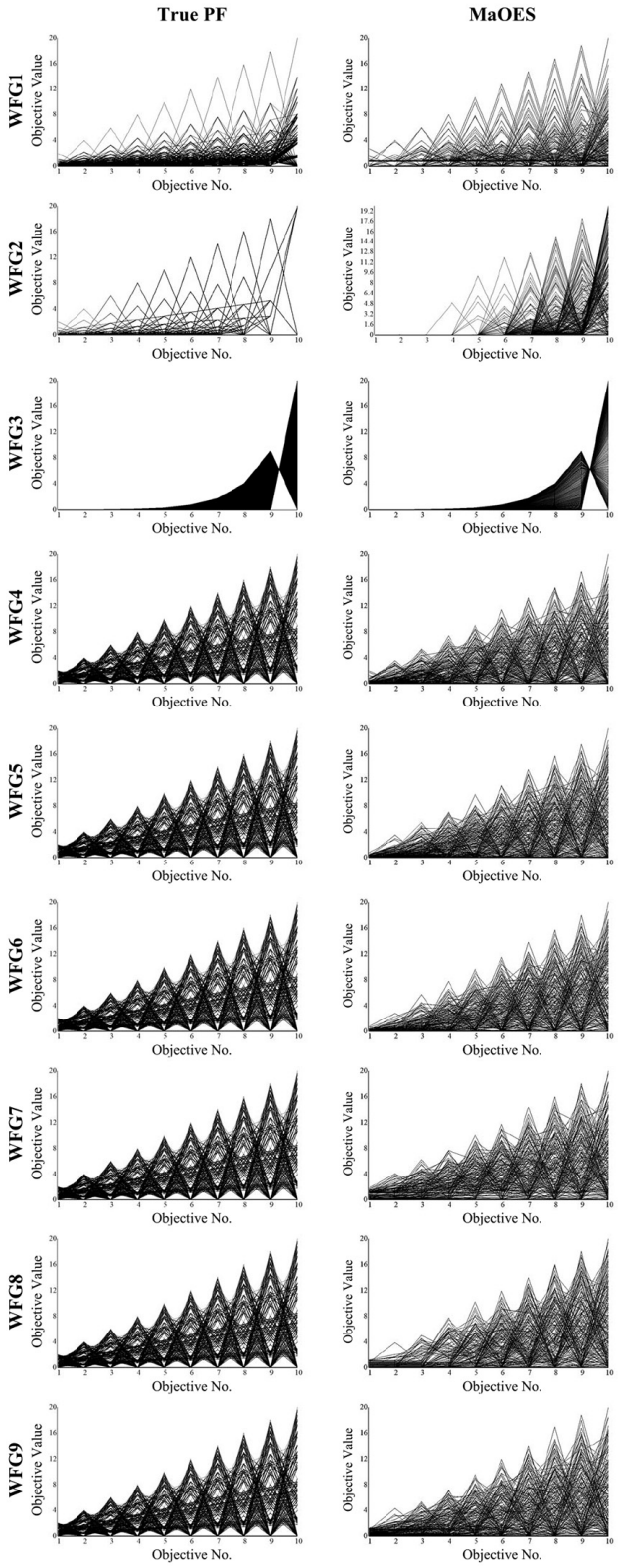

Fig. 11. Solution sets obtained by MaOES and true PF on the ten-objective WFG test suite through parallel coordinates.

Fig. 12 shows the corresponding parallel coordinates of the solutions of five state-of-the-art MaOEAs along with the PFs on ten-dimension DTLZ1, DTLZ7, WFG3, and WFG4 test instances, which characterized by linear, discontinues, degenerated, and concave PFs.

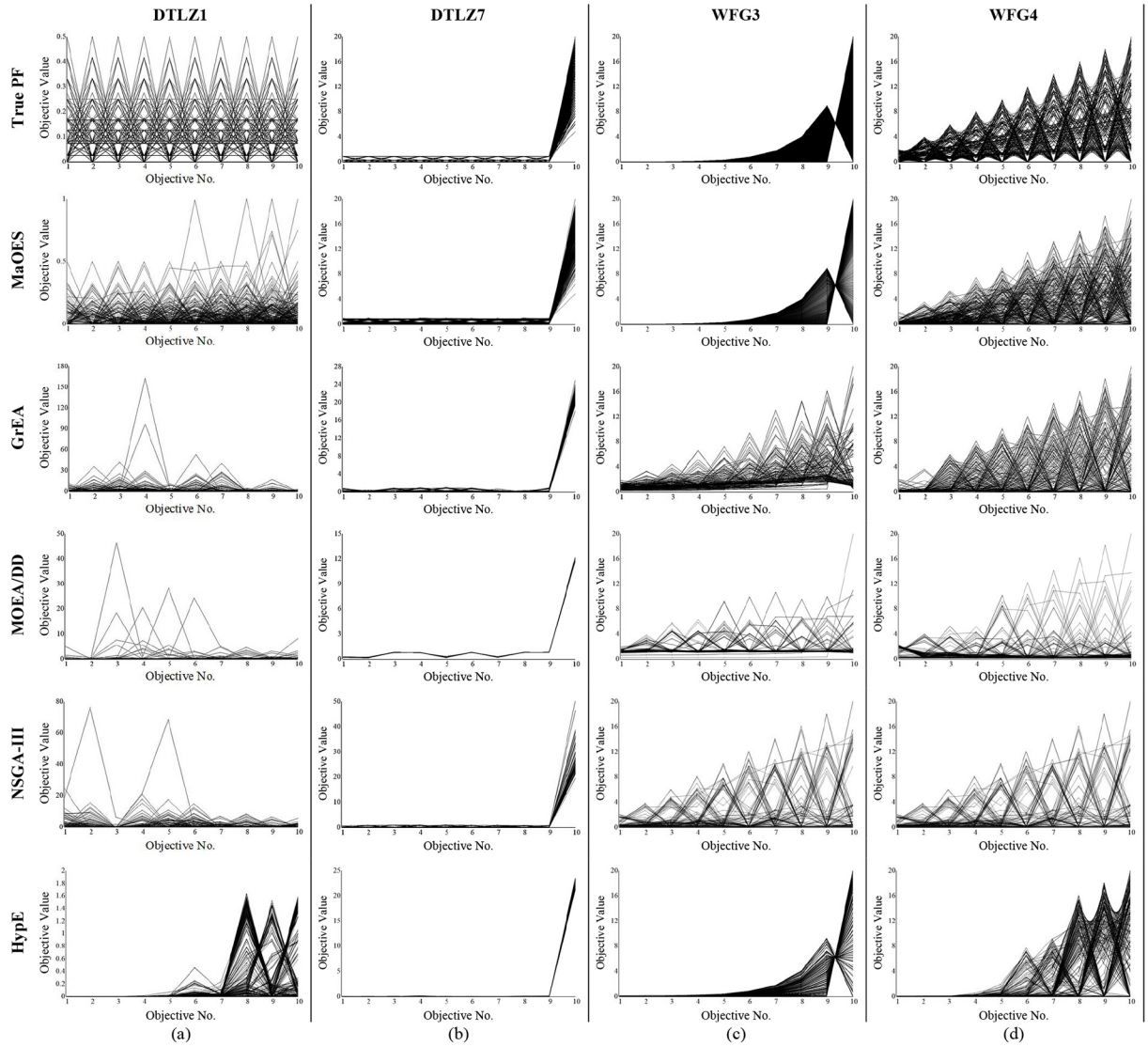

Fig. 12. Solution sets obtained by MaOES, GrEA, MOEA/DD, NSGAIII, HypE, and true PF on the ten-objective DTLZ1, DTLZ7, WFG3, and WFG4 through parallel coordinates.

As can be seen in Fig. 12(a), the true DTLZ1 PF ranging from 0 to 0.5. MaOES has a good convergence PF ranging from 0 to 1, the other four algorithms show an inferior convergence, with its solution set ranging from 0 to around 180, 50, and 80, respectively. The results of the discontinues DTLZ7 instance is shown in Fig. 12(b), MaOES performs well on convergence and coverage within the DTLZ7 PF. However, MOEA/DD and HypE fail to cover the region on almost all ten objectives, and GrEA and NSGA-III obtain poor diversity on the first nine objectives.

From Fig. 12(c), MaOES and HypE perform well on convergence and coverage, and MaOES obtains more uniform distribution in all ten objectives. The other three algorithms show an inferior convergence on the degenerated WFG3 PF. In Fig. 12(d), all the algorithms have good convergence on the WFG4 concave PF. The MaOES, GrEA and NSGA-III can reach on all the objectives, however, MOEA/DD and HypE fail to cover the region on two different objectives and five different objectives, respectively. Moreover, the solutions of MaOES and GrEA can spread over the whole range for each objective. In contrast, MOEA/DD and NSGAIII obtain very few lines distributed around the middle section on all the objectives.

From 64 test instances of the DTLZ and WFG benchmark problems, it is clear that MaOES is the best optimizer as it wins 56 instances against NMPSO, wins 59 instances against S3-CMA-ES and onebyoneEA, wins 60 instances against GrEA, wins 61 instances against HypE, wins 62 instances against MyO-DEMR and RPD-NSGAII, and wins 63 instances against NSGA-III. Thus, from the empirical results on DTLZ and WFG test problems, we find that MaOES outperforms other compared MaOEAs.

C. Performance on Different Population Size

The MaOES need not maintain a large population size, since the Maximum Extension Distance can guide the individuals to maintain uniform distances from the nearest neighbors and extend the entire objective space automatically. In fact, the MaOES can efficiently obtain quality converged and diversified solutions which cover the entire true PF with

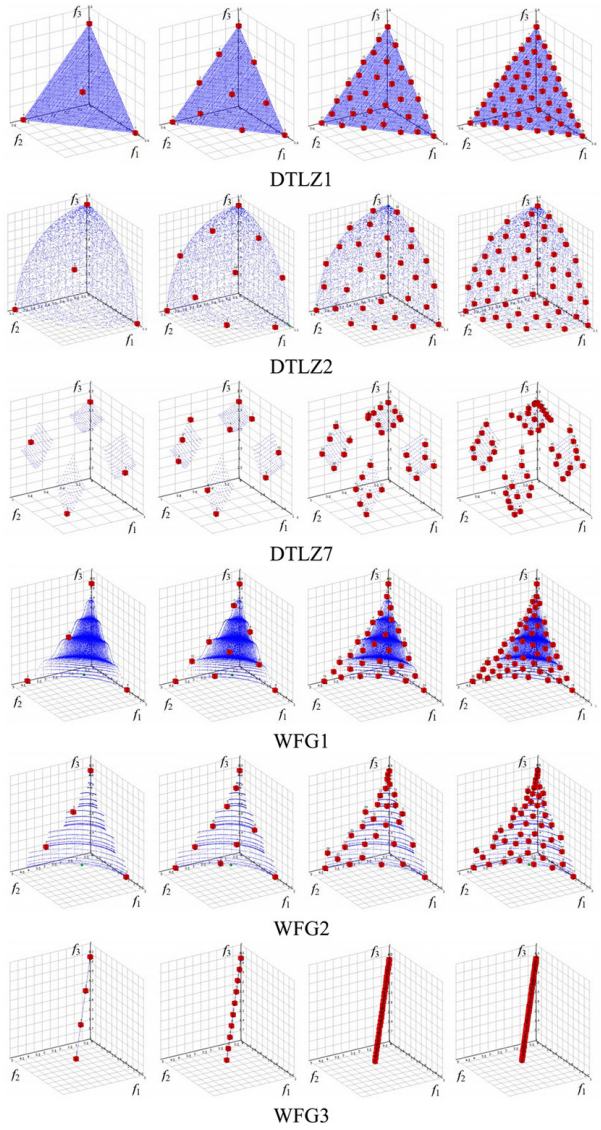

Fig. 13. Experimental results for selected benchmark functions with different population sizes by MaOES (i.e., 4, 10, 30, and 50).

various population sizes (i.e., 4, 10, 30, and 50) as shown in Fig. 13.

V. Conclusion

In this article, we proposed an ES for solving MaOPs based on ES. The algorithm imitates the isotropic magnetic particles, which automatically repel each other and extend the entire magnetic fields as far as possible. In the proposed algorithm, an efficient self-adaptive Precision Controllable Mutation operator was designed for individuals to explore and exploit the decision space. In addition, the Maximum Extension Distance strategy was designed to guide individuals to keep uniform distances and extension to approximate the entire PF automatically. The MaOES can obtain a well-converged and well-diversified PF with much less population size and far lower computational complexity. The larger the number of individuals, the sharper the contour of the approximate PF will be.

The performance is compared against nine different categories of state-of-the-art MaOEAs, including GrEA, NSGA-III, MOEA/DD, HypE and RPD-NSGAII, S3-CMA-ES, MyO-DEMR, NMPSO, and onebyone EA. The experimental results show that MaOES provides the best IGD measure, and the performance of the proposed algorithm is significantly better than the chosen competing MaOEAs on DTLZ and WFG with 3–10 objectives. The results demonstrate the ability of our MaOES to deal with the problems characterized by linear, concave, mixed convex and concave, disconnected convex, and degenerated MaOPs.

Compared with the existing MaOEAs, our algorithm has satisfactorily addressed several challenges.

1) Since every mutated new solution x' needs only compare with its original individual x, there is no selection pressure and dominance resistance problem in our algorithm.
2) In our algorithm, individuals like isotropic magnetic particles, would repel from each other, and keep uniform distance from the nearest neighbors. Our MaOES can obtain well-diversified solutions without explicit diversity preservation scheme.
3) The proposed Maximum Extension Distance strategy is the product of NearDist() and TotalDist(). The greater the maximum extension distance implies an individual has extended the overall boundary and better individual diversity. Our MaOES can extend to approximate the entire PF automatically without explicitly identifying or keeping the boundary or extreme solutions.
4) The overall computational complexity of one generation of MaOES is equal to $O(MP^2)$. In addition, the experimental results show that the MaOES needs only very little population size to obtain a well-converged and well-diversified PF. The larger the number of individuals, the sharper the contour of the approximate PFs will be.
5) MaOES requires no reference points or sensitive parameters, and the experimental results show that MaOES is very robust to deal with linear, concave, mixed convex and concave, disconnected convex, and degenerated MaOPs.
6) Given the required search precision, the Precision-Controllable Mutation operator can generate a new mutated solution for both exploration and exploitation efficiently. The Precision-Controllable Mutation operator can improve the efficiency and eliminate unnecessary computational cost.

References

[1] K. Deb, A. Pratap, S. Agarwal, and T. Meyarivan, "A fast and elitist multiobjective genetic algorithm: NSGA-II," *IEEE Trans. Evol. Comput.*, vol. 6, no. 2, pp. 182–197, Apr. 2002.

[2] E. Zitzler, M. Laumanns, and L. Thiele, "SPEA2: Improving the strength Pareto evolutionary algorithm," in *Proc. Evol. Methods Design Optim. Control Appl. Ind. Problems (EUROGEN)*, Athens, Greece, 2001, pp. 95–100.

[3] P. J. Fleming, R. C. Purshouse, and R. J. Lygoe, "Many-objective optimization: An engineering design perspective," in *Proc. Int. Conf. Evol. Multi Criterion Optim.*, 2005, pp. 14–32.

[4] J. G. Herrero, A. Berlanga, and J. M. M. López, "Effective evolutionary algorithms for many-specifications attainment: Application to air traffic control tracking filters," *IEEE Trans. Evol. Comput.*, vol. 13, no. 1, pp. 151–168, Feb. 2009.

[5] K. Narukawa and T. Rodemann, "Examining the performance of evolutionary many-objective optimization algorithms on a real-world application," in *Proc. 6th Int. Conf. Genet. Evol. Comput.*, Kitakushu, Japan, 2012, pp. 316–319.

[6] A. Sülflow, N. Drechsler, and R. Drechsler, "Robust multi-objective optimization in high dimensional spaces," in *Proc. Int. Conf. Evol. Multi Criterion Optim.*, Matsushima, Japan, 2007, pp. 715–726.

[7] S. X. Yang, M. Q. Li, X. H. Liu, and J. H. Zheng, "A grid-based evolutionary algorithm for many-objective optimization," *IEEE Trans. Evol. Comput.*, vol. 17, no. 5, pp. 721–736, Oct. 2013.

[8] Z. He, G. G. Yen, and J. Zhang, "Fuzzy-based Pareto optimality for many-objective evolutionary algorithms," *IEEE Trans. Evol. Comput.*, vol. 18, no. 2, pp. 269–285, Apr. 2014.

[9] K. Deb and H. Jain, "An evolutionary many-objective optimization algorithm using reference-point-based nondominated sorting approach, Part I: Solving problems with box constraints," *IEEE Trans. Evol. Comput.*, vol. 18, no. 4, pp. 577–601, Aug. 2014.

[10] K. Li, K. Deb, Q. Zhang, and S. Kwong, "An evolutionary many-objective optimization algorithm based on dominance and decomposition," *IEEE Trans. Evol. Comput.*, vol. 19, no. 5, pp. 694–716, Oct. 2015.

[11] J. Bader and E. Zitzler, "HypE: An algorithm for fast hypervolume-based many-objective optimization," *Evol. Comput.*, vol. 19, no. 1, pp. 45–76, 2011.

[12] H. K. Singh, A. Isaacs, and T. Ray, "A Pareto corner search evolutionary algorithm and dimensionality reduction in many-objective optimization problems," *IEEE Trans. Evol. Comput.*, vol. 15, no. 4, pp. 539–556, Aug. 2011.

[13] H. Chen, R. Cheng, J. Wen, H. Li, and J. Weng, "Solving large-scale many-objective optimization problems by covariance matrix adaptation evolution strategy with scalable small subpopulations," *Inf. Sci.*, vol. 509, no. 1, pp. 457–469, 2020.

[14] I. Rechenberg, *Evolution Strategy: Optimizing Technical Systems With Principles of Biological Evolution (in German)*. Stuttgart, Germany: Frommann-Holzboog, 1973.

[15] H. Schwefel, *Numerical Optimization of Computer Models Using Evolutionary Strategy*. Basel, Switzerland: Birkhauser Verlag, 1977.

[16] J. Zhang, X. Yuan, Z. Zeng, B. P. Buckles, C. Koutsougeras, and S. Amer, "Niching in an ES/EP context," in *Proc. Congr. Evol. Comput.*, Washington, DC, USA, 1999, pp. 1426–1433.

[17] O. Takahashi and S. Kobayashi, "An adaptive neighboring search using crossover-like mutation for multi modal function optimization," in *Proc. IEEE Int. Conf. Syst. Man Cybern.*, Tucson, AZ, USA, 2001, pp. 261–267.

[18] O. Aichholzer *et al.*, "Evolution strategy and hierarchical clustering," *IEEE Trans. Magn.*, vol. 38, no. 2, pp. 1041–1044, Mar. 2002.

[19] C.-H. Im, H.-K. Kim, H.-K. Jung, and K. Choi, "A novel algorithm for multimodal function optimization based on evolution strategy," *IEEE Trans. Magn.*, vol. 40, no. 2, pp. 1224–1227, Mar. 2004.

[20] J. Knowles and D. Corne, "The Pareto archived evolution strategy: A new baseline algorithm for Pareto multiobjective optimisation," in *Proc. Congr. Evol. Comput.*, Washington, DC, USA, 1999, pp. 98–105.

[21] R. Fuller, *Synergetics—Explorations in the Geometry of Thinking*, vol. 1. New York, NY, USA: Macmillan, 1975.

[22] R. Fuller, *Synergetics—Explorations in the Geometry of Thinking*, vol. 2. New York, NY, USA: Macmillan, 1979,

[23] Q. Lin *et al.*, "Particle swarm optimization with a balanceable fitness estimation for many-objective optimization problems," *IEEE Trans. Evol. Comput.*, vol. 22, no. 1, pp. 32–46, Feb. 2018.

[24] R. Denysiuk, L. Costa, and I. E. Santo, "Many-objective optimization using differential evolution with variable-wise mutation restriction," in *Proc. 15th Annu. Conf. Genet. Evol. Comput.*, Amsterdam, The Netherlands, 2013, pp. 591–598.

[25] Y. Liu, D. Gong, J. Sun, and Y. Jin, "A many-objective evolutionary algorithm using a one-by-one selection strategy," *IEEE Trans. Cybern.*, vol. 47, no. 9, pp. 2689–2702, Sep. 2017.

[26] D. Gong, J. Sun, and Z. Miao, "A set-based genetic algorithm for interval many-objective optimization problems," *IEEE Trans. Evol. Comput.*, vol. 22, no. 1, pp. 47–60, Feb. 2018.

[27] K. Deb, M. Mohan, and S. Mishra, "Evaluating the ϵ-domination based multi-objective evolutionary algorithm for a quick computation of Pareto-optimal solutions," *Evol. Comput.*, vol. 13, no. 4, pp. 501–525, 2005.

[28] M. Li, S. Yang, and X. Liu, "Shift-based density estimation for Pareto-based algorithms in many-objective optimization," *IEEE Trans. Evol. Comput.*, vol. 18, no. 3, pp. 348–365, Jun. 2014.

[29] M. Elarbi, S. Bechikh, A. Gupta, L. B. Said, and Y.-S. Ong, "A new decomposition-based NSGA-II for many-objective optimization," *IEEE Trans. Syst., Man, Cybern., Syst.*, vol. 48, no. 7, pp. 1191–1210, Jul. 2018.

[30] H. Ishibuchi, Y. Setoguchi, H. Masuda, and Y. Nojima, "Performance of decomposition-based many-objective algorithms strongly depends on Pareto front shapes," *IEEE Trans. Evol. Comput.*, vol. 21, no. 2, pp. 169–190, Apr. 2017.

[31] E. Zitzler and S. Künzli, "Indicator-based selection in multiobjective search," in *Proc. 8th Int. Conf. Parallel Problem Solving Nat.*, Birmingham, U.K., 2004, pp. 832–842.

[32] D. K. Saxena, J. A. Duro, A. Tiwari, K. Deb, and Q. Zhang, "Objective reduction in many-objective optimization: Linear and nonlinear algorithms," *IEEE Trans. Evol. Comput.*, vol. 17, no. 1, pp. 77–99, Feb. 2013.

[33] E. Mezura-Montes and C. A. Coello Coello, "A simple evolution strategy to solve constrained optimization problems," in *Proc. Genet. Evol. Comput. Conf.*, Chicago, IL, USA, 2003, pp. 640–641.

[34] T. Salimans, J. Ho, X. Chen, and I. Sutskever, "Evolution strategies as a scalable alternative to reinforcement learning," *arXiv preprint arXiv:1703.03864*, 2017. [Online]. Available: https://arxiv.org/abs/1703.03864v2

[35] R. C. Purshouse and P. J. Fleming, "On the evolutionary optimization of many conflicting objectives," *IEEE Trans. Evol. Comput.*, vol. 11, no. 6, pp. 770–784, Dec. 2007.

[36] J. Knowles and D. Corne, "Quantifying the effects of objective space dimension in evolutionary multiobjective optimization," in *Proc. Int. Conf. Evol. Multi Criterion Optim.*, Matsushima, Japan, 2007, pp. 757–771.

[37] H. Ishibuchi, N. Tsukamoto, and Y. Nojima, "Evolutionary many-objective optimization: A short review," in *Proc. IEEE Congr. Evol. Comput. (CEC)*, Hong Kong, 2008, pp. 2419–2426.

[38] B. Li, J. Li, K. Tang, and X. Yao, "Many-objective evolutionary algorithms: A survey," *ACM Comput. Surveys*, vol. 48, no. 1, pp. 1–35, 2015.

[39] H.-G. Beyer and H.-P. Schwefel, "Evolution strategies: A comprehensive introduction," *Nat. Comput.*, vol. 1, no. 1, pp. 3–52, 2002.

[40] K. Deb and R. B. Agrawal, "Simulated binary crossover for continuous search space," *Complex Syst.*, vol. 9, no. 2, pp. 115–148, 1995.

[41] S. Huband, L. Barone, L. While, and P. Hingston, "A scalable multi-objective test problem toolkit," in *Proc. Int. Conf. Evol. Multi Criterion Optim.*, Guanajuato, Mexico, 2005, pp. 280–295.

[42] K. Deb, L. Thiele, M. Laumanns, and E. Zitzler, "Scalable test problems for evolutionary multiobjective optimization," in *Evolutionary Multi-Objective Optimization, Advanced Information and Knowledge Processing*. London, U.K.: Springer, 2005, pp. 105–145.

[43] Y. Tian, R. Cheng, X. Zhang, and Y. Jin, "PlatEMO: A MATLAB platform for evolutionary multi-objective optimization [educational forum]," *IEEE Comput. Intell. Mag.*, vol. 12, no. 4, pp. 73–87, Nov. 2017.

[44] P. Czyzak and A. Jaszkiewicz, "Pareto simulated annealing-a metaheuristic technique for multiple-objective combinatorial optimization," *J. Multi Criteria Decis. Anal.*, vol. 7, no. 1, pp. 34–47, 1998.

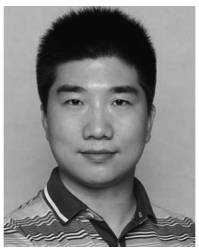

Kai Zhang received the Ph.D. degree in system analyses and integration from the Huazhong University of Science and Technology, Wuhan, China, in 2008.

He was a Postdoctoral Research Fellow with the School of Electronics Engineering and Computer Science, Peking University, Beijing, China, from 2008 to 2010. He is currently a Professor with the School of Computer Science and Technology, Wuhan University of Science and Technology, Wuhan. His research focuses on evolutionary computation and multicriteria decision making.

Zhiwei Xu received the B.S. degree in information security from the Wuhan University of Science and Technology, Wuhan, China, in 2017, where he is currently pursuing the Ph.D. degree with the School of Computer Science and Technology.

His research interests include evolutionary computation and many-objective optimization.

Shengli Xie (Fellow, IEEE) received the M.S. degree in mathematics from Central China Normal University, Wuhan, China, in 1992, and the Ph.D. degree in control theory and applications from the South China University of Technology, Guangzhou, China, in 1997.

He is currently a Full Professor and the Head of the Key Laboratory of Intelligent Detection and The Internet of Things in Manufacturing, Guangdong University of Technology, Guangzhou. He has authored or coauthored 2 books and over 200 scientific papers in journals and conference proceedings. His research interests include wireless networks, automatic control, and blind signal processing.

Prof. Xie was a recipient of the Second Prize in China's State Natural Science Award in 2009 for his research on blind source separation and identification.

Gary G. Yen (Fellow, IEEE) received the Ph.D. degree in electrical and computer engineering from the University of Notre Dame, Notre Dame, IN, USA, in 1992.

He was with the Structure Control Division, U.S. Air Force Research Laboratory, Albuquerque, NM, USA. In 1997, he joined Oklahoma State University, Stillwater, OK, USA, where he is currently a Regents Professor with the School of Electrical and Computer Engineering. His research interests include intelligent control, computational intelligence, conditional health monitoring, and signal processing and their industrial/defense applications.

Dr. Yen received the Andrew P Sage Best Transactions Paper Award from the IEEE Systems, Man and Cybernetics Society in 2011 and the Meritorious Service Award from the IEEE Computational Intelligence Society in 2014. He was an Associate Editor of the *IEEE Control Systems Magazine*; the IEEE TRANSACTIONS ON CONTROL SYSTEMS TECHNOLOGY; *Automatica*; *Mechantronics*; the IEEE TRANSACTIONS ON SYSTEMS, MAN, AND CYBERNETICS—PART A; the IEEE TRANSACTIONS ON SYSTEMS, MAN, AND CYBERNETICS—PART B; and the IEEE TRANSACTIONS ON NEURAL NETWORKS. He is currently serving as an Associate Editor for the IEEE TRANSACTIONS ON EVOLUTIONARY COMPUTATION and the IEEE TRANSACTIONS ON CYBERNETICS. He served as the General Chair for the 2003 IEEE International Symposium on Intelligent Control, Houston, TX, USA, and the 2006 IEEE World Congress on Computational Intelligence, Vancouver, BC, Canada. He served as the Vice President for the Technical Activities from 2005 to 2006 and the President from 2010 to 2011 of the IEEE Computational intelligence Society. He is the Founding Editor-in-Chief of *IEEE Computational Intelligence Magazine* from 2006 to 2009. He is a fellow of IET.